Ultrafast Photodetectors with Near-unity Quantum Efficiency

G. Ulu [a], M. Gökkavas, M. S. Ünlü [b]
N. Bıyıklı, E. Özbay [c], O. Aytür [d]
R. P. Mirin and D. H. Christensen [e]

[a]Department of Physics,
[b] Department of Electrical and Computer Engineering, Boston University, Boston, MA 02215

[c]Department of Physics,
[d] Department of Electrical Engineering, Bilkent University, Ankara, Turkey, 06533.

[e]National Standards and Technology, Boulder, CO 80303.

ABSTRACT

We designed, fabricated and characterized $Al_xGa_{1-x}As/GaAs$ p-i-n resonant cavity enhanced (RCE) photodetectors with near-unity quantum efficiency. The peak wavelength is in the 780-830 nm region and post-process adjustable by recessing the top surface. Transit time limited bandwidth for these devices is in excess of 50 GHz. Possible applications of these detectors include conventional measurements of low light levels, quantum optical experiments that use pulsed sources and short-haul high speed communications.

Keywords: quantum efficiency, near-unity, nearly unit, RCE, photodetector

1. INTRODUCTION

Optical communications has been the traditional driving force of photodetector research. Local-area networks and short-distance communications have a growing demand for fast and efficient detectors to complement vertical-cavity surface-emitting lasers (VCSELs) in the 800-1000 nm range. VCSELs have emerged as the preferred sources owing to their tunability and high modulation-bandwidth.[1–3] Photodetectors with bandwidths up to 100 GHz and efficiencies up to 90 % have been demonstrated for this purpose in the 800-1000 nm wavelength range.[4,5] Beside communications, quantum optics also requires high-speed photodetectors with high quantum efficiencies (η). The outcomes of optical experiments that involve measurements of the fluctutations and correlations of light beams in the quantum regime depend on the quantum efficiencies of the photodetectors. For example, the amount of quantum noise reduction observed with intensity-correlated twin beams[6,7] has been actually limited by η. An "imperfect" detector mixes the vacuum modes with the signal modes at the point of detection, which can also be interpreted as the introduction of a "partitioning noise". For η less than unity, the relation between the intrinsic quantum observables and the statistics of fluctuations become complicated. Thus any realistic extraction of information from detection schemes such as a homodyne setup has to compensate for sub-unity η of the detectors.[8,9] In addition to perfect efficiency, fast temporal response is also called for, as pulsed sources are widely used in order to enhance interactions in the nonlinear media involved in these experiments. A typical source in the 800-1000 nm range is a mode-locked Ti:sapphire laser which provides light pulses a few picoseconds wide at repetition rates of 80 MHz.

In this work, we describe theoretical and experimental studies of ultrafast resonant-cavity-enhanced (RCE) photodetectors with quantum efficiencies approaching unity for quantum optical applications.

Other author information: (Send correspondence to G. Ulu)
G. Ulu : E-mail: ulu@bu.edu

Part of the SPIE Conference on Photodetectors: Materials and Devices IV
San Jose, California • January 1999
SPIE Vol. 3629 • 0277-786X/99/$10.00

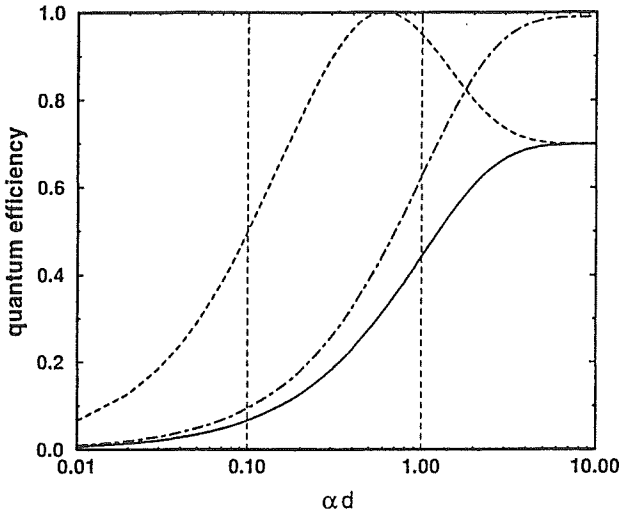

Figure 1. The dependence of η on absorption path in a conventional (solid) and RCE (dashed) detector with $R_{top} = 0.3$ and $R_{bottom} = 0.99$ (the reflectance of the bottom mirror). The dot-dashed line shows a conventional detector with perfect antireflection coating.

2. DEVICE DESIGN AND FABRICATION

The quantum efficiency of a conventional detector is,

$$\eta = (1 - R_{top})\,[1 - \exp(-\alpha d)] \tag{1}$$

where α is the absorption coefficient for an absorption layer of thickness d and R_{top} is the reflectance of the top surface. It is possible to build conventional detectors with very high η provided that R_{top} is eliminated by anti-reflection (AR) coating. However, the thick absorption regions would limit the high speed performance due to long transit times of the photogenerated carriers. Furthermore, thick active layers are hard to deplete and cause further limitation because of diffusion from the undepleted absorbing regions. On the other hand, high η values can be attained by RCE photodetection with relatively thin active layers due to the enhancement of the optical field in the active layer placed inside a Fabry-Perot cavity.[10] Figure 1 shows a comparison of conventional and RCE photodetectors in terms of dependence of peak η on the parameter αd. For a RCE detector with the GaAs-air interface as the top mirror, $\eta > 0.99$ can be achieved in a finite range of αd values around 0.65, corresponding to an absorption layer thickness an order of magnitude less than that for a conventional device with perfect AR coating.[10] In addition to reducing transit times, small absorption paths also eliminate secondary carrier recombination that could further limit η. Finally, another important feature of RCE detectors is that their resonance wavelengths can be adjusted by recessing the top surface of the device.

Figure 2 depicts the cross-section of our device design. The epilayer structure was grown by solid-source molecular beam epitaxy on a semi-insulating GaAs substrate. An $Al_{0.2}Ga_{0.8}As/GaAs$ p-i-n detector is placed in a low loss Fabry-Perot resonator formed by the semiconductor-air interface as the top mirror and a distributed Bragg reflector (DBR) as the bottom mirror. The DBR mirror consists of 24 quarter-wave stacks of $Al_{0.2}Ga_{0.8}As/AlAs$. Its stop band is designed for > 99 % reflectance in a 40 nm wavelength window centered around 820 nm. The active layer is 470 nm of intrinsic GaAs. The interfaces between the absorption layer and the doped regions are alloy-graded to avoid carrier trapping. The thickness is chosen according to the optimization: $R_{top} = R_{bottom}\exp(-2\alpha d)$.[10] We used scattering-matrix methods to calculate the reflectance and quantum efficiency of our designs.

In Fig. 3, we plot the calculated and measured reflectance at the center of the as-grown wafer where the closest match to the design structure is reached with a 1% reduction in the thicknesses of the DBR layers. Reflectance measurements performed on the edges of the wafer indicated that the layer thicknesses deviate down to 96% of their target values. This point was also confirmed by the fact that the resonance wavelength shifted to shorter wavelengths

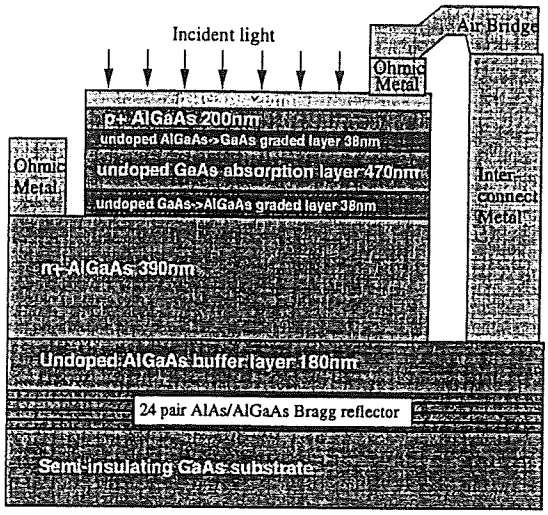

Figure 2. The cross-section of the device reveals the epilayer structure. Use of airbridges reduces parasitic capacitances.

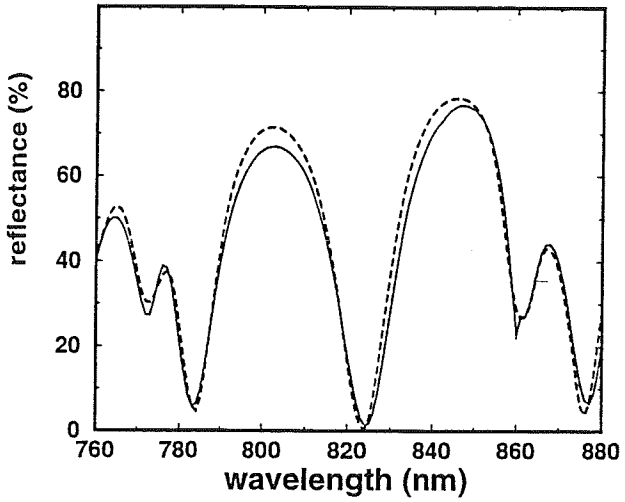

Figure 3. The graph shows the measured reflectance of the as-grown wafer (solid line) and the calculated reflectance (dashed) taking into account a 1% reduction in DBR layer thicknesses.

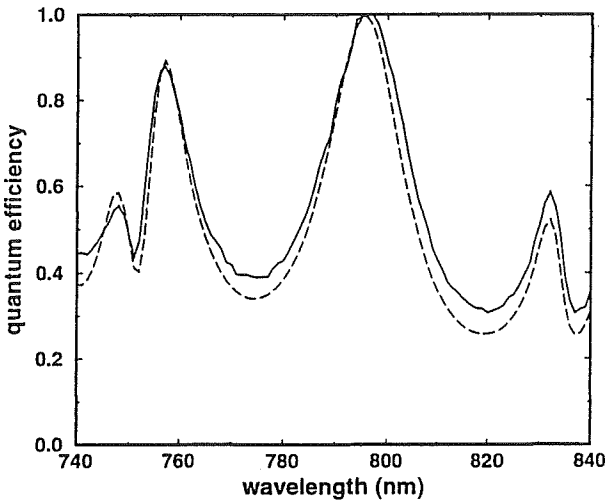

Figure 4. The quantum efficiency data from a 250 μm $\times$ 250 μm detector. The dotted line is the simulation fit to the data taking into account possible structural deviations.

on the samples near the edges of the wafer. In our simulations, we included a linear average of the reflectance values over the finite size of the probe beam.

The devices were fabricated by a microwave-compatible process described elsewhere.[4] To optimize high-speed performance, we formed coplanar waveguides on the substrate. Airbridges made of 1 μm thick gold connect the center of the waveguides to the ohmic contacts of the device with minimal parasitic capacitance. The breakdown voltages of the photodiodes were over 14 V. The dark current in a 30 μm diameter device was 20 pA.

3. MEASUREMENTS

3.1. Quantum Efficiency

To characterize quantum efficiencies approaching unity, it is essential to collect all of the excitation on the device under test. We used a tunable continuous wave Ti:sapphire laser and single mode fibers for light delivery onto the detectors. In earlier measurements, we used a monochromated tungsten-halogen lamp coupled into a multimode fiber.[4] But those measurements were limited by poor spatial confinement in the core and light lost in cladding modes. In our current setup, the low numerical aperture of the single-mode fiber yields a narrow circular beam, allowing for uniform illumination of small devices at normal incidence without bringing the fiber very close to the surface. For device sizes on the order of the optical mode in the fiber, a very small fiber-to-sample distance is required resulting in an optical cavity formation and causing an interference pattern. The output from the laser was split to provide a reference beam to track the laser power fluctuations.

In Fig. 4, we plot the measured and calculated quantum efficiency of a 250 μm $\times$ 250 μm detector that exhibits unity efficiency at 800 nm. The accuracy of our measurements on large area devices was $\pm 2\%$ and was only limited by the responsivity data (supplied by the manufacturer) of the NIST-traceable detector used to calibrate the setup. We estimate two main sources of deviation between the measured and calculated results: One being the lack of reliable absorption data for GaAs, the other being the variations of layer thicknesses over the wafer during the growth, especially of the DBR mirror as mentioned above. Figure 5 demonstrates the tunability of our devices after the fabrication by slow recess etches. The peaks preserve their finesse and efficiency along the tuning range determined by the stop band of the bottom mirror.

The results shown were recorded with no bias across the device. In fact, the spectral responses are not altered by application of reverse bias, indicating that the entire active layer is fully depleted by the built-in field.

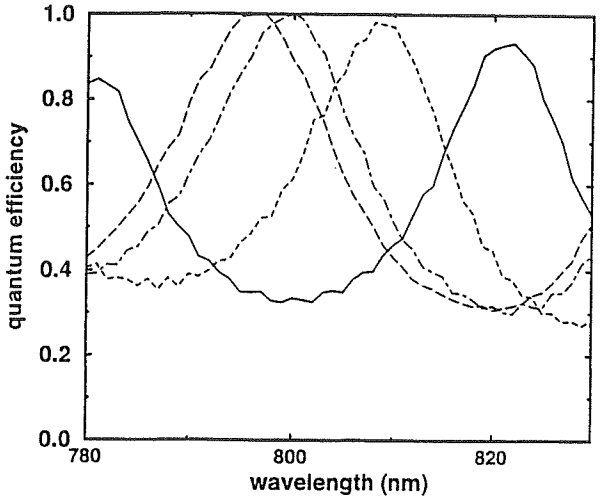

Figure 5. The resonance wavelength shifts toward shorter wavelengths as the top surface is recessed. The η of as-grown wafer (solid line) is sub-unity, because the GaAs cap layer is not removed yet.

3.2. High-speed performance

We have already mentioned that high bandwidth is necessary for applications utilizing pulsed sources. A careful consideration of the temporal response of the photodetector is appropriate for another reason: At extremely low light levels, detectors operate in photon counting mode. The statistics of a certain observable of the field is described by discrete arrival times of individual photons, each of which generate a single current pulse. At high light levels, the detector operates in analog mode where photocurrent is measured. Since the photocurrent is made up of many current pulses, it encodes the fluctuations of the field. Indeed, the photocurrent is a convolution of photon arrival times with the impulse response of the device. To preserve the maximum information, high-bandwidth is necessary but not sufficient. An impulse response that is short and with less spread in time would preserve the information of the photon arrival times to a greater extent. Minimization of diffusion spread, which often can not be indicated by bandwidth, is therefore also important.

We used a microwave probe station with a 50 GHz sampling oscilloscope and a mode-locked picosecond Ti:sapphire laser as the excitation. The smallest devices (14 μm $\times$ 8 μm) exhibited the fastest response governed by the transit time in the absorption region. A temporal response of 12 ps full-width-at half-maximum (FWHM) is shown in Fig.6. The measurement of these devices were limited by the speed of the sampling oscilloscope. When the response of the scope and excitation pulse width is deconvolved, the estimated 3-dB bandwidth is more than 50 GHz.

Figure 7 illustrates the normalized responses of several devices with varying sizes. For larger devices, the depletion capacitance is appreciable. The depletion capacitance is 0.25 fF/μm^2 corresponding to a f_{3dB-RC} of 10 GHz for a 40 μm $\times$ 40 μm device with R = 50 Ω.

As in efficiency measurements, the temporal responses were independent of the external bias and the results are shown for zero bias. We again deduce that the intrinsic absorption regions were fully depleted with built-in voltage. Since the carriers are generated in the absorption region which is fully covered by the field, all of them are collected via drift process. Thus no diffusion process is involved in the response.

We also observed in large devices that the sheet resistance of the top p^+ layer induces a finite risetime if the recess etch removes a significant portion of the doped layer. This effect becomes more pronounced as the beam size is reduced relative to the device size. The thickness and the p^+ doping have to be chosen to make allowance for tuning etches without compromising the temporal response.

In contrast to RCE detectors, a conventional Si p-i-n photodetector would require a 50 μm thick absorption layer for near-unity efficiency at this wavelength region. The transit time would be 1-2 ns if the device could be fully

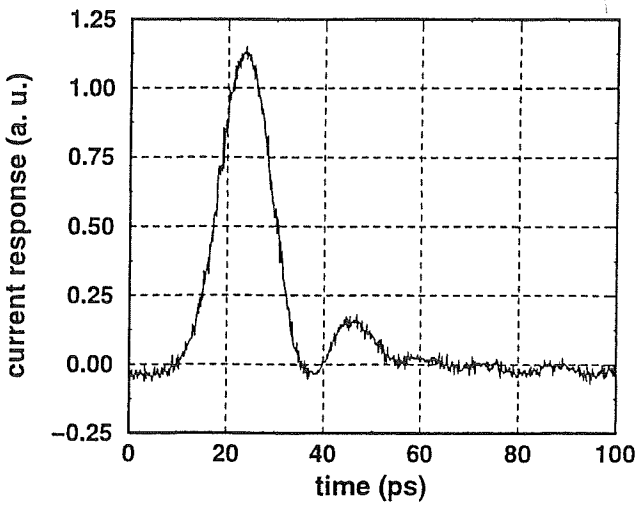

Figure 6. Temporal response of a device exhibiting $\tau_{\mathrm{FWHM}} = 12$ ps.

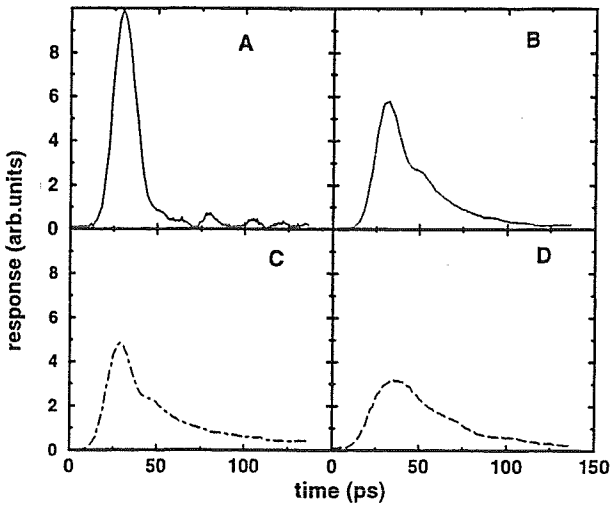

Figure 7. High speed responses from small and large devices. An RC tail evolves as the active area gets larger. A: 14 μm $\times$ 8 μm, and the diameters of the round detectors B, C, D are 30 μm, 60 μm, and 100 μm respectively.

depleted. In the likely case of incomplete depletion, the diffusion of photogenerated carriers in the neutral regions would further degrade the time response. Given the long diffusion length of Si, almost all of the carriers within the penetration depth of the optical excitation would reach the contacts resulting in a diffusion tail of many nanoseconds in the photocurrent. Therefore the bandwidth for a conventional p-i-n with near-unity η is in the MHz regime.

4. CONCLUSION

In conclusion, we designed, fabricated and characterized high-speed RCE photodetectors with near-unity quantum efficiency. The bandwidth-efficiency products of the detectors are in excess of 50 GHz. The resonance wavelengths were post-process adjustable in the spectral region 780-830 nm. The deviations from the design were shown to be the

result of errors in crystal growth calibration. To the best of our knowledge, these devices are the fastest photodetectors with $\eta > 0.99$ measured to an accuracy of 2%. Picosecond temporal response combined with adjustable-wavelength near-unity η makes these RCE detectors suitable for quantum optical experiments, especially those with pulsed lasers.

5. ACKNOWLEDGEMENTS

This work was supported by the Office of Naval Research Grant N00014-96-10652, the National Science Foundation International Collaborative Research Grant INT-9601770, and the Turkish Scientific and Technical Council Project No. EEEAG-156.

REFERENCES

1. A. K. Dutta, H. Kosaka, K. Kurihara, Y. Sugimoto, and K. Kasahara, "High-speed vcsel of modulation bandwidth over 7.0 ghz and its application to 100 m pcf datalink," *IEEE J. Lightwave Technol.* **16**, pp. 870–875, 1998.
2. K. M. Hanson in *IEEE LEOS 1997 Annual Meeting*, LEOS, ed., *LEOS 97 Conference Proceedings* **2**, pp. 419–420, 1997.
3. P. Tayebati, P. Wang, D. Vakhshoori, C. Lu, M. Azimi, and R. N. Sacks, "Half-symmetric cavity tunable microelectromechanical vcsel with single spatial mode," *IEEE Photon. Techol. Lett.* **10**, pp. 1679–1681, 1998.
4. E. Özbay, N. Bıyıklı, I. Kimukin, O. Aytür, M. Gökkavas, G. Ulu, R. Mirin, D. Christensen, and M. S. Ünlü, "High-speed > 90% quantum-efficiency p-i-n photodiodes with a resonance wavelength adjustable in 795-835 nm range.," *Appl. Phys. Lett.* **to be published in**, 1999.
5. B. M. Onat, M. Gokkavas, E. Özbay, E. P. Ata, E. Towe, and M. S. Ünlü, "100-ghz resonant cavity enhanced schottky photodiodes," *IEEE Photonics Tech. Lett.* **10**, pp. 707–709, 1998.
6. P. Kumar and O. Aytür, "Squeezed-light generation with an incoherent pump," *Phys. Rev. Lett.* **64**, pp. 1015–1018, 1990.
7. O. Aytür and P. Kumar, "Pulsed twin beams of light," *Phys. Rev. Lett.* **65**, pp. 1551–1554, 1990.
8. K. Banaszek, "Maximum-likelihood estimation of photon-number distribution from homodyne statistics," *Phys. Rev. A* **57**, pp. 5013–5015, 1998.
9. K. Banaszek and K. Wodkiewicz, "Operational theory of homodyne detection," *Phys. Rev. A.* **55**, pp. 3117–3123, 1997.
10. M. S. Ünlü and S. Strite, "Resonant cavity enhanced photonic devices," *J. Appl. Phys.* **78**, pp. 607–628, 1995.